X-ray generation from relativistic electrons passing through thin targets in cyclical accelerators

N.N. Nasonov [a,*], A.S. Kubankin [a], V.V. Kaplin [b], S.R. Uglov [b], M.A. Piestrup [c], C.K. Gary [c]

[a] *Laboratory of Radiation Physics, Belgorod State University, 14 Studencheskaya str., Belgorod 308007, Russia*
[b] *Nuclear Physics Institute, Tomsk Polytechnic University, P.O. Box 25, Tomsk 634050, Russia*
[c] *Adelphi Technology Inc., 981-B Industrial Road, San Carlos, CA 94070, USA*

Abstract

The characteristics of quasi-monochromatic tunable X-ray sources based on multipasses of electrons through thin targets installed in cyclical accelerators are discussed. An internal bremsstrahlung radiator coupled with a multilayer X-mirror placed outside the accelerator vacuum chamber is used to produce tunable, narrow spectra. It is compared with other radiators using different emission mechanisms, such as transition radiation and coherent bremsstrahlung. The calculated formulae given here allow the comparison of the spectral and angular-distribution intensities of these mechanisms.

© 2004 Elsevier B.V. All rights reserved.

1. Introduction

The efficiency of X-ray sources based on relativistic electron emission in condensed media is limited by the effect of photoabsorption. The reduction of absorption by the installation of thin targets, where the thickness of the target is less than the photoabsorption length, into a circular accelerator has been demonstrated experimentally [1–3].

There are a variety of possible coherent and incoherent emission mechanisms that permit recycling through thin radiators. For example, quasi-monochromatic fluxes of soft and hard X-rays can be produced by the parametric X-ray radiation (PXR) from relativistic electrons crossing a crystalline target [4–6]. The main defect of such a mechanism is the small emission intensity. The same is true for diffracted transition radiation from relativistic electrons crossing a crystal [7]. A more intense source can be created using ordinary transition radiation from relativistic electrons crossing an amorphous target. But this source produces a wide spectrum of emitted photons and requires an electron beam of very high energy in order to produce hard X-rays.

Higher intensity PXR can be achieved when a multilayer X-mirror is used [8–12]. The limitation on the intensity of such a source occurs when hard

* Corresponding author. Tel.: +7-22-341477; fax: +7-22-341692.
E-mail address: nnn@bsu.edu.ru (N.N. Nasonov).

X-ray generation is required, and very small orientation angles between an emitting particle velocity and reflecting plane of X-mirror are required. The path of the electrons through the multilayer is then large, and the resulting increase in multiple scattering of the emitting electrons increases the spectral width and decreases the total yield of the emitted photons.

Thus, these two problems appear to be intrinsic in the coherent mechanisms of X-ray emission from relativistic electrons in condensed media: high energy electrons are needed for hard X-ray generation and the yield is restricted primarily by the multiple scattering of the emitting electrons. To overcome these issues, a simple and effective X-ray radiator is considered here consisting of a thin amorphous target, installed in a circular accelerator, and an X-mirror placed outside the accelerator's chamber. Ordinary bremsstrahlung, emitted from relativistic electrons in amorphous target, is reflected by X-mirror in this scheme. There are definite advantages of a bremsstrahlung radiator: (1) the spectrum is very wide, and therefore one can use electrons with relatively modest energies for the production of hard X-rays; (2) bremsstrahlung is less sensitive to multiple scattering in comparison with coherent X-ray emission mechanisms; (3) since emitting electrons do not interact with the X-mirror, small orientation angles between bremsstrahlung flux and the X-mirror plane are possible; (4) since the X-mirror reflects photons in a wider frequency range than that a crystal, the intensity can exceed that of a source based on PXR from a crystal.

The main goal of this work is to calculate the spectral and angular characteristics of the photon flux emitted from such a source and to compare them with the parameters of an X-mirror. The required energy of the emitting electrons and the number of passes that they make through such targets are compared. Only the process of X-ray producing during the interaction of the emitting electron with a radiator is studied here without account of X-ray photoabsorption in a vacuum window between the accelerator chamber and external X-mirror.

In our search for high-intensity radiators for cyclical accelerators, we will also consider the use of thin amorphous internal targets for the generation of transition radiation as well as the use of oriented crystalline targets for coherent bremsstrahlung production. The increase in X-ray yield from crystalline radiators in comparison with amorphous ones has been observed experimentally [13,14].

In Section 2 the general formula for the emission spectral–angular distribution is derived considering both bremsstrahlung and transition radiation production. The relevant features of X-ray emission for the case of a modest energy electron beam, when the emission yield is determined primarily by bremsstrahlung, are described in Section 3. The case of higher energy electrons, where transition radiation dominates, is considered in Section 4. Coherent bremsstrahlung is considered in Section 5. Our conclusions are presented in Section 6.

2. The emission spectral–angular distribution

Let us consider an X-ray source as shown in Fig. 1. Here an electron beam crosses a thin target along the axis $\mathbf{e}_1$. Emitted photons propagate along this axis striking an X-mirror with the thickness $N_0 T$ (T is the period of X-mirror, N_0 is the number of periods) placed parallel to the plane $x = 0$. The axis $\mathbf{e}_2$ is oriented along the X-ray detector's axis. The emission angle φ is usually fixed. The orientation angle Θ', relative to the position of exact Bragg resonance, describes the rotation of the X-mirror by a goniometer.

The Fourier-transform of the emission field $\mathbf{E}_{\omega\mathbf{k}} = (2\pi)^{-4} \int dt \, d^3 r \mathbf{E}(\mathbf{r}, t) \exp(i\omega t - i\mathbf{kr})$ in X-mirror is calculated using the X-ray dynamical diffraction theory [15]

$$(k^2 - \omega^2(1 + \chi_0))\mathbf{E}_{\omega\mathbf{k}} - \mathbf{k}(\mathbf{k}\mathbf{E}_{\omega\mathbf{k}})$$
$$- \omega^2 \sum_{\mathbf{g}}{}' \chi_{-\mathbf{g}}\mathbf{E}_{\omega\mathbf{k}+\mathbf{g}} = 0, \qquad (1)$$

where χ_0 and $\chi_{\mathbf{g}}$ are the coefficients in the Fourier-transform of X-mirror dielectric susceptibility $\chi(\omega, \mathbf{r}) = \chi_0(\omega) + \sum_{\mathbf{g}}{}' \chi_{\mathbf{g}}(\omega) e^{i\mathbf{gr}}$, $\mathbf{g}$ is the reciprocal lattice vector, $g = 2\pi n/T$, $n = \pm 1, \pm 2, \ldots$ The quantities χ_0 and $\chi_{\mathbf{g}}$ are determined by
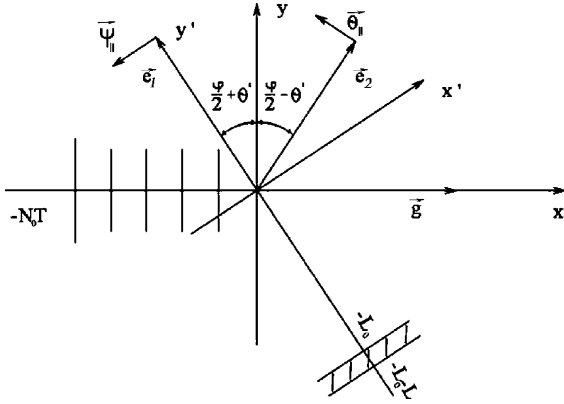
Fig. 1. The principal scheme of X-ray source. Here $\mathbf{e}_1$ is the electron beam axis, $\mathbf{e}_2$ is the X-ray detector axis, φ is the fixed emission angle, θ' is the orientation angle describing the rotation of the X-mirror by the use of a goniometer, L is the thickness of the target, N_0T is the thickness of X-mirror, T is its period, $\mathbf{g}$ is the reciprocal lattice vector, the angular components $\Psi_\parallel$ and $\theta_\parallel$ describe the electron beam spread and the emitted photon angular distribution respectively.

$$\chi_0 = \frac{a}{T}\chi_a + \frac{b}{T}\chi_b, \quad \chi_\mathbf{g} = \frac{1-e^{iga}}{igT}(\chi_a - \chi_b),$$
$$\chi_{a,b} = -\frac{\omega_{a,b}^2}{\omega^2} + i\chi''_{a,b},$$

(2)

where χ_a and χ_b are the dielectric susceptibilities of alternate layers in X-mirror, a and b are the thicknesses of these layers, and ω_a and ω_b are the plasma frequencies of corresponding layers.

Two wave approximation equations

$$(k^2 - \omega^2(1+\chi_0))E_{\lambda 0} - \omega^2\chi_{-\mathbf{g}}\alpha_\lambda E_{\lambda\mathbf{g}} = 0,$$
$$(k_\mathbf{g}^2 - \omega^2(1+\chi_0))E_{\lambda\mathbf{g}} - \omega^2\chi_\mathbf{g}\alpha_\lambda E_{\lambda 0} = 0,$$

(3)

following from (1) have the well-known solution

$$E_{\lambda 0} = a_\lambda\delta(\xi - \xi_1) + b_\lambda\delta(\xi - \xi_2),$$
$$E_{\lambda\mathbf{g}} = \frac{(\omega^2/2p)\chi_\mathbf{g}\alpha_\lambda}{\xi - (\omega^2/2p)\chi_0}E_{\lambda 0},$$

(4)

where the following definitions are used:

$$\mathbf{E}_{\omega\mathbf{k}} \approx \sum_{\lambda=1}^{2}\mathbf{e}_{\lambda 0}E_{\lambda 0}, \quad \mathbf{E}_{\omega\mathbf{k}+\mathbf{g}} \approx \sum_{\lambda=1}^{2}\mathbf{e}_{\lambda\mathbf{g}}E_{\lambda\mathbf{g}},$$
$$\mathbf{e}_{10} = \mathbf{e}_{1\mathbf{g}} = \frac{[\mathbf{k}_\parallel\mathbf{e}_x]}{k_\parallel}, \quad \mathbf{e}_{20} = \frac{[\mathbf{k}\mathbf{e}_{10}]}{k}, \quad \mathbf{e}_{2\mathbf{g}} = \frac{[\mathbf{k}_\mathbf{g}\mathbf{e}_{10}]}{k_\mathbf{g}},$$

$$\mathbf{k}_\mathbf{g} = \mathbf{k} + \mathbf{g} = \mathbf{k}_\parallel + \mathbf{e}_x k_{gx}, \quad k_{gx} = p + \xi,$$
$$\xi \ll p = \sqrt{\omega^2 - k_\parallel^2},$$
$$\Delta = g\left(\frac{g}{2p} - 1\right) \ll g, \quad \alpha_1 = 1, \quad \alpha_2 = \cos\varphi,$$
$$\xi_{1,2} = \frac{1}{2}\left(\Delta \pm \sqrt{\left(\Delta - \frac{\omega^2}{p}\chi_0\right)^2 - \frac{\omega^4}{p^2}\chi_\mathbf{g}\chi_{-\mathbf{g}}\alpha_\lambda^2}\right)$$
$$\equiv \frac{1}{2}(\Delta \pm f_\lambda).$$

(5)

The equation for the diffracted emission field $E_{\lambda\mathbf{g}}^{\mathrm{rad}}$ propagating in a vacuum along the axis $\mathbf{e}_2$ (see Fig. 1)

$$(k_g^2 - \omega^2)E_{\lambda\mathbf{g}}^{\mathrm{rad}} \approx 2p\xi E_{\lambda\mathbf{g}}^{\mathrm{rad}} = 0$$

(6)

follows from (3) in the limit $\chi_0 = \chi_\mathbf{g} = \chi_{-\mathbf{g}} = 0$. Using (4), the solution of (6)

$$E_{\lambda\mathbf{g}}^{\mathrm{rad}} = c_\lambda\delta(\xi)$$

(7)

and the ordinary boundary conditions

$$\int d\xi\, e^{-i\xi N_0 T} E_{\lambda\mathbf{g}} = \int d\xi(E_{\lambda\mathbf{g}} - E_{\lambda\mathbf{g}}^{\mathrm{rad}})$$
$$= \int d\xi(E_{\lambda 0} - E_{\lambda 0}^{\mathrm{inc}}) = 0$$

(8)

one can express the unknown coefficient c_λ in terms of the incident field $E_{\lambda 0}^{\mathrm{inc}}$ propagating in a vacuum behind the internal target along the axis $\mathbf{e}_1$ (see Fig. 1)

$$c_\lambda = d_\lambda R_\lambda, \quad d_\lambda = \int_{-\infty}^{+\infty} d\xi E_{\lambda 0}^{\mathrm{inc}},$$
$$R_\lambda = \left(\frac{\omega^2}{p}\chi_\mathbf{g}\alpha_\lambda\left[\exp\left(\frac{i}{2}f_\lambda N_0 T\right) - \exp\left(-\frac{i}{2}f_\lambda N_0 T\right)\right]\right)$$
$$\Big/\left(\left(\Delta + f_\lambda - \frac{\omega^2}{p}\chi_0\right)\exp\left(\frac{i}{2}f_\lambda N_0 T\right)\right.$$
$$\left. - \left(\Delta - f_\lambda - \frac{\omega^2}{p}\chi_0\right)\exp\left(-\frac{i}{2}f_\lambda N_0 T\right)\right),$$

(9)

where the quantity f_λ denotes the radical in the formula for $\xi_{1,2}$ in (5).

For further analysis it is necessary to determine the incident field $E_{\lambda 0}^{\mathrm{inc}}$. To determine this, let us find

solutions to the wave equation for the field inside the internal target

$$(k^2 - \omega^2(1 + \chi))E_{\lambda 0} = \frac{i\omega e}{4\pi^3} \int dt \mathbf{e}_{\lambda 0} \mathbf{v}_e e^{i\omega t - i\mathbf{k}\mathbf{r}_e}, \quad (10)$$

where χ is the dielectric susceptibility of internal target, $\mathbf{v}_e(t) = d\mathbf{r}_e/dt$ is the velocity of an emitting electron. The solutions to the field in the vacuum in front and behind the internal target follow from (10) in the limit $\chi = 0$. Using known methods, one obtains the following expression for $E_{\lambda 0}^{inc}$:

$$E_{\lambda 0}^{inc} = p_\lambda \delta\left(k_y' - \sqrt{\omega^2 - k_\parallel'^2}\right)$$
$$+ \frac{i\omega e}{4\pi^3} \frac{1}{k^2 - \omega^2} \int dt \mathbf{e}_{\lambda 0} \mathbf{v}_e e^{i\omega t - i\mathbf{k}\mathbf{r}_e}, \quad (11)$$

where the coefficient p_λ is determined as

$$p_\lambda = \frac{i\omega e}{4\pi^3} \int_{-\infty}^{+\infty} dk_y'$$
$$\times \left(\frac{1}{k_y'^2 - \omega^2(1 + \chi) + k_\parallel'^2} - \frac{1}{k_y'^2 - \omega^2 + k_\parallel'^2}\right)$$
$$\times \left(1 - e^{-i\left(k_y' - \sqrt{\omega^2(1+\chi) - k_\parallel'^2}\right)L}\right)$$
$$\times e^{-i\left(k_y' - \sqrt{\omega^2 - k_\parallel'^2}\right)L_0} \int dt \mathbf{e}_{\lambda 0} \mathbf{v}_e e^{i\omega t - i\mathbf{k}\mathbf{r}_e} \quad (12)$$

and k_y' and $\mathbf{k}_\parallel'$ are the corresponding components of the vector $\mathbf{k}$ in the system of coordinates $x'y'$ (see Fig. 1).

Results (9), (11), and (12) allow us to obtain a comprehensive description of emission characteristics. In order to obtain an emission amplitude it is necessary to calculate the Fourier integral

$$E_\lambda^{rad} = \int d^3 k_g e^{i\mathbf{k}_g \mathbf{n}r} E_{\lambda 0}^{rad} \rightarrow A_\lambda \frac{e^{i\omega r}}{r},$$
$$A_\lambda = -2\pi i \omega n_x c_\lambda|_{\mathbf{k}_\parallel = \omega \mathbf{n}_\parallel}, \quad \mathbf{n} = \mathbf{n}_\parallel + \mathbf{e}_x n_x, \quad \mathbf{e}_x \mathbf{n}_\parallel = 0.$$
$$(13)$$

The integration in (13) was done using the stationary phase method. Here $\mathbf{n}$ is the unit vector to the direction of an emitting particle propagation. It is convenient to express $\mathbf{n}$ in terms of a two-dimensional observation angle $\mathbf{\Theta}$ in accordance with the formula

$$\mathbf{n} = \mathbf{e}_2\left(1 - \frac{1}{2}\Theta^2\right) + \mathbf{\Theta}, \quad \mathbf{e}_2\mathbf{\Theta} = 0. \quad (14)$$

Using the definition (14), one can obtain from (9), (11) and (12) the general expression for the emission spectral–angular distribution of emitted photons

$$\omega \frac{dN_\lambda}{d\omega d^2\Theta} = \langle|A_\lambda|^2\rangle,$$
$$A_\lambda = \frac{i\omega e}{2\pi}\left[e^{-i\frac{\omega L}{2}}\int_L^\infty dt \mathbf{e}_{\lambda 0} \mathbf{v}_e e^{i\omega\sigma_0}\right.$$
$$\left. + \int_0^L dt \mathbf{e}_{\lambda 0} \mathbf{v}_e e^{i\omega\sigma_*} + \int_{-\infty}^0 dt \mathbf{e}_{\lambda 0} \mathbf{vee}^{i\omega\sigma_0}\right]R_\lambda,$$
$$\sigma_0 = t - \Theta_\perp z_e(t) - (2\Theta' + \Theta_\parallel)x_e'(t)$$
$$- \left(1 - \frac{1}{2}\Theta_\perp^2 - \frac{1}{2}(2\Theta' + \Theta_\parallel)^2\right)y_e'(t),$$
$$\sigma_* = \sigma_0 - \frac{1}{2}\chi y_e'(t),$$
$$(15)$$

where the brackets $\langle \rangle$ mean averaging over all the possible particle trajectories $\mathbf{r}_e'(t) = \mathbf{e}_z z_e(t) + \mathbf{e}_y' y_e'(t) + \mathbf{e}_x' x_e'(t)$. When integrating over dk_y' and $d\xi$ in (9) and (12), it is necessary to get around the poles correctly.

The result (15) takes into account both bremsstrahlung and transition radiation contributions as well as an interference between those radiation fields that can be very important [16,17]. For our purposes it is sufficient to consider two limiting cases corresponding to a predominance of only one of the mentioned mechanisms. It should be noted that the trajectory $\mathbf{r}_e(t)$ is not determined in (15). Therefore this expression describes both ordinary bremsstrahlung from an amorphous target as well as coherent bremsstrahlung from a crystalline target.

3. X-ray source based on the diffracted bremsstrahlung

Let us consider emission from electrons of relatively small energies $\varepsilon = \gamma m \ll m\omega/\omega_0$ (or $\varepsilon \leqslant$ tens MeV for ω of the order of tens keV), m is the electron mass, ω_0 is the plasma frequency of

the internal target and $\chi = -\omega_0^2/\omega^2$. It is important that the energy of emitted photons ω is approximately constant because the X-mirror extracts the photons with energies in the vicinity of the Bragg frequency only. Assuming the condition $\omega\chi L \ll 1$ to be valid, one can obtain for the emission amplitude A_λ the very simple expression

$$A_\lambda^{\mathrm{br}} = \frac{\mathrm{i}\omega e}{2\pi} \int_{-\infty}^{+\infty} \mathrm{d}t \mathbf{e}_{\lambda 0} \mathbf{v}_e \, \mathrm{e}^{\mathrm{i}\omega\sigma_0} R_\lambda \equiv \mathrm{d}_\lambda R_\lambda. \qquad (16)$$

For thin internal targets $L \ll L_{\mathrm{sc}} \approx \frac{\mathrm{e}^2}{4\pi} L_R$ (L_R is the radiation length), the multiple scattering angle $\Theta_{\mathrm{sc}} \approx \gamma^{-1}\sqrt{L/L_{\mathrm{sc}}}$ is small relative to the characteristic emission angle $\Theta_{\mathrm{em}} \approx \gamma^{-1}$ [18], and the dipole approximation of the emission theory is valid. For this approximation the particle's velocity $\mathbf{v}_e$ is assumed to be constant. Defining the angular variable $\boldsymbol{\Psi}$ by the formulae

$$\mathbf{v} = \mathbf{e}_1\left(1 - \frac{1}{2}\gamma^{-2} - \frac{1}{2}\Psi^2\right) + \boldsymbol{\Psi}, \quad \mathbf{e}_1\boldsymbol{\Psi} = 0 \qquad (17)$$

one can obtain from (16) by the integration by parts the formulae

$$
\begin{aligned}
\mathrm{d}_1 &= \frac{e}{\pi} \frac{1}{\gamma^{-2} + \Omega^2} \int \mathrm{d}t \exp\left[\frac{\mathrm{i}\omega}{2}(\gamma^{-2} + \Omega^2)t\right] \\
&\quad \times \left\{\left(1 - \frac{2\Omega_1^2}{\gamma^{-2} + \Omega^2}\right)W_z - \frac{2\Omega_1\Omega_2}{\gamma^{-2} + \Omega^2}W_x'\right\}, \\
\mathrm{d}_2 &= \frac{e}{\pi} \frac{1}{\gamma^{-2} + \Omega^2} \int \mathrm{d}t \exp\left[\frac{\mathrm{i}\omega}{2}(\gamma^{-2} + \Omega^2)t\right] \\
&\quad \times \left\{\left(1 - \frac{2\Omega_2^2}{\gamma^{-2} + \Omega^2}\right)W_x' - \frac{2\Omega_1\Omega_2}{\gamma^{-2} + \Omega^2}W_z\right\},
\end{aligned}
$$
$$(18)$$

where $\Omega_1 = \Theta_\perp - \Psi_\perp$, $\Omega_2 = 2\Theta' + \Theta_\parallel + \Psi_\parallel$, $\Omega^2 = \Omega_1^2 + \Omega_2^2$, W_z and W_x' are the transversal components of the particle's acceleration in the system of coordinates $x'y'z$ (see Fig. 1).

The acceleration $\mathbf{W}$ can be expressed in terms of potentials of atoms, located in the internal target

$$\mathbf{W} = \frac{\mathrm{i}e}{m\gamma} \int \mathrm{d}^3k(\mathbf{k} - \mathbf{v}\cdot\mathbf{k}\mathbf{v})\varphi_{-\mathbf{k}}\mathrm{e}^{-\mathrm{i}\mathbf{k}\mathbf{v}t} \sum_\alpha \mathrm{e}^{\mathrm{i}\mathbf{k}\mathbf{r}_\alpha}, \qquad (19)$$

where $\varphi_{\mathbf{k}}$ is the Fourier-transform of the potential of a single atom, $\mathbf{r}_\alpha$ is the coordinate of αth atom in internal target. In the case of an amorphous target,

$\mathbf{r}_\alpha$ is uniformly distributed over the volume of the target.

The final expression for the spectral–angular distribution of the diffracted bremsstrahlung intensity, following from (15)–(19), has the simple form

$$
\begin{aligned}
\omega\frac{\mathrm{d}^4 N_\lambda^{\mathrm{br}}}{\mathrm{d}t\,\mathrm{d}\omega\,\mathrm{d}^2\Theta} &\approx \frac{8Z^2\mathrm{e}^6 n_0 \ln(mR)}{\pi m^2\gamma^2} \\
&\times \left\langle \frac{1}{(\gamma^{-2} + \Omega^2)^2}\left(1 - \frac{4\gamma^{-2}\Omega_\lambda^2}{(\gamma^{-2} + \Omega^2)^2}\right)|R_\lambda|^2\right\rangle,
\end{aligned}
$$
$$(20)$$

where Z is the atomic number, n_0 is the density of atoms in the internal target, and R is the screening radius in the Fermi–Thomas atom model. The brackets $\langle \ \rangle$ designate averaging over the electron beam angular spread as described by the angle $\boldsymbol{\Psi}$. It is important that this averaging is unrelated to reflection coefficient $|R_\lambda|^2$.

The spectral–angular distribution of the total photon flux, emitted after n passes of the electron beam through an internal target, follows from (20),

$$
\begin{aligned}
\omega\frac{\mathrm{d}^3 N_\lambda^{\mathrm{br}}}{\mathrm{d}\omega\,\mathrm{d}^2\Theta} &= \frac{8Z^2\mathrm{e}^6 n_0 \ln(mR)}{\pi m^2\gamma^2} \sum_{l=1}^{n} P_l F_\lambda^{(l)}|R_\lambda|^2, \\
F_\lambda^{(l)} &= \frac{1}{\pi} \int_0^L \mathrm{d}t \exp\left(-\frac{L-t}{L_{\mathrm{ab}}}\right) \int \frac{\mathrm{d}^2\Psi}{\Psi_l^2 + t/\gamma^2 L_{\mathrm{sc}}} \\
&\quad \times \exp\left(-\frac{\Psi^2}{\Psi_l^2 + t/\gamma^2 L_{\mathrm{sc}}}\right) \\
&\quad \times \frac{1}{(\gamma^{-2} + \Omega^2)^2}\left(1 - \frac{4\gamma^{-2}\Omega_\lambda^2}{(\gamma^{-2} + \Omega^2)^2}\right),
\end{aligned}
$$
$$(21)$$

where P_l is the probability for an electron to undergo the lth collision in the internal target. P_l is the monotonically decreasing function of the number of passes l; one can introduce the average number of passes $\langle n \rangle$, so that $P_l \approx 1$ for $l < \langle n \rangle$ and $P_l \ll 1$ for $l \gg \langle n \rangle$, the values of $\langle n \rangle$ are determined by specific properties of the internal target and circular accelerator. L_{ab} is the photo-absorption length, $\Psi_l^2 = \Psi_0^2 + (L/\gamma^2 L_{\mathrm{sc}})(l - 1)$, and Ψ_0 is the initial angular spread of the electron beam.

The spectrum of the emission is completely determined by the function R_λ from (9). Analyzing the properties of this function, one should take into account that the photoabsorption in the X-mirror, which is not as important as the case of PXR where the photoabsorption determines the maximum emission yield [11]. Thus, the influence of the photoabsorption can be neglected if a photoabsorption length exceeds the X-mirror's extinction length (such a condition is always valid). A very simple expression for $|R_\lambda|^2$ follows from (9) under such conditions

$$|R_\lambda|^2 = \frac{|\sinh^2(\delta_\lambda\sqrt{1-\tau_\lambda^2(\omega)})|}{|1-\tau_\lambda^2(\omega)| + |\sinh^2(\delta_\lambda\sqrt{1-\tau_\lambda^2(\omega)})|},$$
(22)

where the function $\tau_\lambda(\omega)$ is defined by the expression

$$\tau_\lambda = \frac{g^2}{2\omega_g^2|\alpha_\lambda|}\left(1 + 2\frac{\omega_p^2}{g^2} - \frac{2\omega n_x}{g}\right)$$

$$\approx \frac{g^2}{2\omega_g^2|\alpha_\lambda|}\left(1 - \frac{\omega}{\omega_B'}\right),$$
(23)

$$\omega_B' = \omega_B\left(1 + (\Theta' + \Theta_\parallel)\cot\frac{\varphi}{2}\right),$$

$$\omega_B = \frac{g}{2\sin(\varphi/2)}.$$

Here

$$\delta_\lambda = \frac{\omega_g^2}{g}N_0T\alpha_\lambda, \quad \omega_p^2 = \omega_a^2\frac{a}{T} + \omega_b^2\frac{b}{T},$$

$$\omega_g^2 = (\omega_a^2 - \omega_b^2)\frac{\sin(\pi a/T)}{\pi}.$$
(24)

The function $|R_\lambda(\tau_\lambda)|^2$, calculated for different values of the parameter δ_λ, is shown in Fig. 2. Following these curves, the reflected peak is formed in the range $\delta_\lambda > 2$ only, when the number of Be-layers in X-mirror is large:

$$N_0 > N_* = \frac{4\pi^2}{(\omega_a^2 - \omega_b^2)T^2}.$$
(25)

The spectrum of reflected photons is concentrated in the vicinity of a modified Bragg frequency $\omega_B(1 + \Theta'\cot(\varphi/2))$. Its width depends strongly
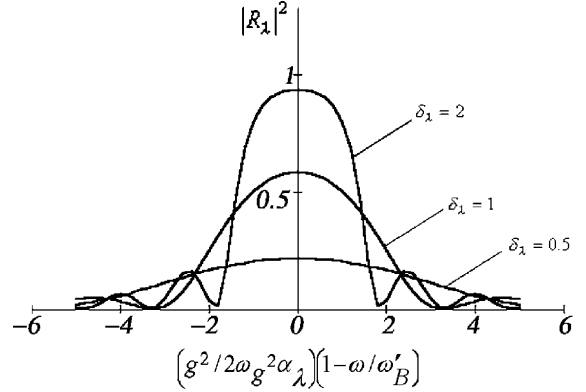

Fig. 2. The dependence of the reflection coefficient $|R_\lambda|^2$ on the X-mirror thickness. Here $\delta_\lambda = \omega_g^2 N_0 T\alpha_\lambda/g$ (see the definitions (23) and (24)).

on the photon collimator angular size $\Delta\Theta_\parallel$ if $\Delta\Theta_\parallel > 1/N_*$. Strongly collimated photon flux ($\Delta\Theta_\parallel < 1/N_*$) has the "natural width"

$$\frac{\Delta\omega}{\omega} \approx \frac{4\omega_g^2|\alpha_\lambda|}{g^2} \approx \frac{(\omega_a^2 - \omega_b^2)T^2}{\pi^3}$$
(26)

determined by X-mirror parameters only.

One of the most important advantages of a diffracted bremsstrahlung source is the possibility of generating hard X-rays by the use of an electron beam of modest energy (e.g. 20 MeV). Since the scale of X-mirror period T has the value of approximately 10 angstroms, a very small reflection angle φ (see Fig. 1) is needed for hard X-ray generation, following from the expression for the Bragg frequency ω_B in (13). The polarization coefficient $\alpha_2 = \cos\varphi \approx 1 = \alpha_1$ and the reflection coefficient $|R_\lambda(\delta_\lambda, \tau_\lambda)|^2$ do not depend on the polarization index λ because $\delta_1 \approx \delta_2 = \delta = (\omega_g^2/g)N_0T$ and $\tau_1 \approx \tau_2 = \tau = (g^2/2\omega_g^2)(1 - \omega/\omega_B')$.

Assuming that the angular spread of the electron-beam is not changed appreciably for electrons passing through an internal target ($\Theta_{sc}^2 = L/\gamma^2 L_{sc} \ll \Psi_0^2$), assuming the simplest case $n < \langle n \rangle$, and using integration instead of summation over l in the general formula (21), one can reduce this formula after summation over polarizations to the following expression:

$$\omega \frac{\mathrm{d}^3 N^{\mathrm{br}}}{\mathrm{d}\omega \mathrm{d}^2 \Theta} \approx \frac{\mathrm{e}^2}{\pi^2} \frac{L_{\mathrm{ab}}}{L}(1 - \mathrm{e}^{-L/L_{\mathrm{ab}}})$$

$$\times \frac{|\sinh^2(\delta\sqrt{1-\tau^2})|}{|1-\tau^2| + |\sinh^2(\delta\sqrt{1-\tau^2})|}$$

$$\times \int_0^\infty \frac{\mathrm{d}\Psi^2}{(A^2 - B^2)^{3/2}}$$

$$\times \left(A - 2\gamma^{-2}\frac{A^2 + \frac{1}{2}B^2}{A^2 - B^2} + 4\gamma^{-4}A\frac{A^2 + \frac{3}{2}B^2}{(A^2-B^2)^2} \right)$$

$$\times \left(E_1\left(\frac{\Psi^2}{\Psi_0^2 + Ln/\gamma^2 L_{\mathrm{sc}}} \right) - E_1\left(\frac{\Psi^2}{\Psi_0^2} \right) \right),$$
(27)

where

$$A = \gamma^{-2} + \Psi^2 + \Theta^2, \quad B = 2\Psi\Theta,$$
$$\Theta^2 = \Theta_1^2 + \Theta_2^2, \quad \Theta_1 = \Theta_\perp, \quad \Theta_2 = 2\theta' + \Theta_\parallel.$$
(28)

Formula (27) shows a saturation of the described emission yield as a function of the number of passes n due to the influence of multiple scattering of emitting particles. Indeed, the strong dependence of the yield (27) on n occurs for small $n \ll \gamma^2 \Psi_0^2 L_{\mathrm{sc}}/L$, when

$$E_1\left(\frac{\Psi^2}{\Psi_0^2 + Ln/\gamma^2 L_{\mathrm{sc}}} \right) - E_1\left(\frac{\Psi^2}{\Psi_0^2} \right)$$

$$\approx \frac{Ln}{\gamma^2 \Psi_0^2 L_{\mathrm{sc}}} \mathrm{e}^{-\frac{\Psi^2}{\Psi_0^2}} \ll 1,$$
(29)

but such a dependence becomes weak (logarithmic) in the range $n \gg \gamma^2 \Psi_0^2 L_{\mathrm{sc}}/L$. The second case ($n \gg 1$) is more interesting for X-ray generation although one should take into account a finite value of the average number of passes $\langle n \rangle$. To estimate the influence of the finite value of $\langle n \rangle$ let us approximate the probability P_l by the simple function $P_l = \exp(-l/\langle n \rangle)$. Using this approximation and assuming the average multiple scattering angle $\sqrt{L\langle n \rangle/\gamma^2 L_{\mathrm{sc}}}$ to be larger than the initial angular spread Ψ_0, one can obtain in the range $n \gg \langle n \rangle$ from (21) the formula for $\omega \mathrm{d}N^{\mathrm{br}}/\mathrm{d}\omega \mathrm{d}^2\Theta$ different from (27) by the substitution

$$E_1\left(\frac{\Psi^2}{\Psi_0^2 + Ln/\gamma^2 L_{\mathrm{sc}}} \right) - E_1\left(\frac{\Psi^2}{\Psi_0^2} \right)$$

$$\rightarrow 2K_0\left(2\sqrt{\frac{\gamma^2 \Psi^2 L_{\mathrm{sc}}}{L\langle n \rangle}} \right).$$
(30)

This result allows us to determine the maximum possible emission yield.

Let us consider the very important dependence of the yield (27) and (30) on the internal target's atomic number Z. In accordance with (27), the yield is monotonically decreasing function of the ratio L/L_{ab}, and therefore the thickness of internal target L must be less than the absorption length L_{ab}. For example, $L = \frac{1}{2}L_{\mathrm{ab}}$; the factor $(L_{\mathrm{ab}}/L)(1 - \exp(-L/L_{\mathrm{ab}})) \approx 1$ and the Z-dependence of the yield is given by the argument of the Macdonald's function in (30). The average number of passes $\langle n \rangle$ decreases with increasing Z. It is reasonable to assume that $\langle n \rangle \sim L_{\mathrm{sc}} \sim Z^{-2}$. Since $L < L_{\mathrm{ab}} \sim Z^{-4}$, it may be advantageous to use low-Z elements for the internal target because the quantity $\sqrt{\frac{\gamma^2 \Psi^2 L_{\mathrm{sc}}}{L\langle n \rangle}} \sim Z^2$.

Performing the integration over ω in (27) (after the replacement (30)), one obtains the following formula for the angular distribution of emitted photons:

$$\frac{\mathrm{d}^2 N^{\mathrm{br}}}{\mathrm{d}^2 \Theta} \approx \frac{4\mathrm{e}^2 \omega_g^2 \gamma^2}{\pi g^2} \tanh(\delta)\Phi^{\mathrm{br}}\left(\gamma^2\Theta^2, \frac{L\langle n \rangle}{L_{\mathrm{sc}}} \right),$$

$$\Phi^{\mathrm{br}} = \int_0^\infty \frac{\mathrm{d}t K_0\left(2\sqrt{\frac{L_{\mathrm{sc}}}{L\langle n \rangle}t} \right)}{((1+t+\gamma^2\Theta^2)^2 - 4\gamma^2\Theta^2 t)^{\frac{3}{2}}}$$

$$\times \left(1 + t + \gamma^2\Theta^2 - 2\frac{(1+t+\gamma^2\Theta^2)^2 + 2\gamma^2\Theta^2 t}{(1+t+\gamma^2\Theta^2)^2 - 4\gamma^2\Theta^2 t} \right.$$

$$\left. + 2(1+t+\gamma^2\Theta^2)\frac{(1+t+\gamma^2\Theta^2)^2 + 6\gamma^2\Theta^2 t}{((1+t+\gamma^2\Theta^2)^2 - 4\gamma^2\Theta^2 t)^2} \right),$$
(31)

where the quantity ω_g^2 is defined by (24).

In accordance with (31) the angular distribution of diffracted bremsstrahlung is described by the universal function $\Phi^{\mathrm{br}}(\gamma\Theta)$ depending on the one parameter $L\langle n \rangle/L_{\mathrm{sc}}$ only (obviously, this parameter is the ratio of square of average multiple scattering angle $L\langle n \rangle/\gamma^2 L_{\mathrm{sc}}$ to square of characteristic emis-
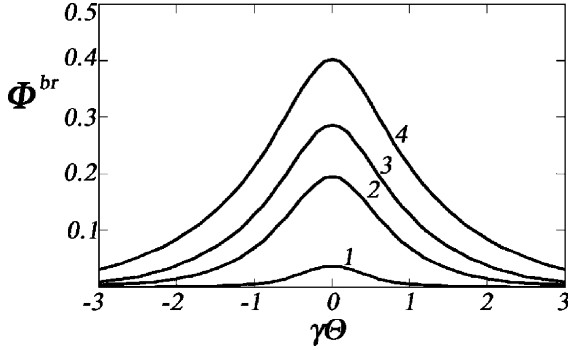
Fig. 3. The bremsstrahlung angular distribution versus the average number of electron passes through an internal target. Here $\frac{d^2 N^{\mathrm{br}}}{d^2 \Theta} = \frac{4e^2 \omega_g^2 \gamma^2}{\pi g^2} \Phi^{\mathrm{br}}$, $\Theta = \sqrt{\Theta_\perp^2 + (2\theta' + \theta_\parallel)^2}$, the curves have been calculated by the formula (31) for different values of the parameter $L\langle n\rangle / L_{\mathrm{sc}} = 0.1$ (curve 1), 1 (curve 2), 2 (curve 3) and 4 (curve 4).

sion angle γ^{-2}). This function is illustrated by the curves in Fig. 3, calculated by (31) for different values of the parameter $L\langle n\rangle / L_{\mathrm{sc}}$.

To estimate the possible intensity of the studied source, let us consider the scheme, containing WB$_4$C multilayer mirror, used in the experiment [9] (the thickness of W-layer $a = 5 \times 10^{-8}$ cm, the thickness of B$_4$C-layer $b = 7 \times 10^{-8}$ cm, the number of periods $N_0 = 300$). In addition to X-mirror parameters, it is necessary to fix the electron energy and the parameters of the internal target. In our estimate we will use the parameters from [19]: the energy of electrons $\epsilon = 33$ MeV, the thickness of beryllium amorphous target $L = 20 \times 10^{-4}$ cm, and the average number of passes $\langle n\rangle = 200$. Using these parameters, one can obtain the following estimation for the angular density of diffracted bremsstrahlung: $d^2 N^{\mathrm{br}}/d^2\Theta \approx 0.14$ ph./el.ster.

The obtained estimation demonstrates the possibility of a tunable quasimonochromatic X-ray source whose brightness can be larger than that of other novel X-ray sources. Indeed, the predicted value of $d^2 N/d^2\Theta$ is comparable with that for PXR source based on the emission from 500 MeV electrons in the multilayer mirror with indicated above parameters (in the last case $d^2 N/d^2\Theta$ in accordance with theoretical predictions made in [11] where an advantage of X-mirror as PXR radiator compared to crystalline one has been

shown) in spite of the fact that the energy of emitting electrons in the case considered (33 MeV) is significantly below.

An emission property of specific interest is the spectrum of emitted photons. The spectral width of strongly collimated photon flux is given by (27) (especially $\Delta\omega/\omega \approx 1\%$ in the case considered). To estimate an influence of the photon collimator size $\Delta\Theta_\parallel$ on the spectral width, let us integrate the general formula (27) (with the replacement (30)) over $\Theta_\perp$ and $\Theta_\parallel$. Since the reflection coefficient $|R|^2$ does not depend on $\Theta_\perp$, the collimator in the form of a slit (collimator angular sizes $\Delta\Theta_\perp$ and $\Delta\Theta_\parallel$ must satisfy the condition $\Delta\theta_\parallel \ll \Delta\Theta_\perp$) seems to be appropriate because of the possible increase in total emission yield without increasing the emission's spectral width. Since the function Φ^{br} is a slowly changing function of observation angles relative to the reflection coefficient, one can integrate over the angle $\theta_\parallel$ in (27) the function $|R|^2$ only. The result of integration, obtained in the case of small enough collimator size $\Delta\theta_\parallel \ll \gamma^{-1}\sqrt{1 + L\langle n\rangle / L_{\mathrm{sc}}}$ is given by

$$\omega \frac{dN^{\mathrm{br}}}{d\omega} \approx \frac{2e^2 \omega_g^2 \gamma \varphi}{\pi^2 g^2} Q^{\mathrm{br}}\left(\frac{\omega}{\omega_{\mathrm{B}}}, \frac{\Delta\theta_\parallel}{\varphi}, 2\gamma\theta', \frac{L\langle n\rangle}{L_{\mathrm{sc}}}\right),$$

$$Q^{\mathrm{br}} = \int_{-\infty}^{+\infty} dy\, \Phi^{\mathrm{br}}(\gamma^2 \Theta^2)$$

$$\times \int_{\tau_-}^{\tau_+} \frac{d\tau |\sinh^2(\delta\sqrt{1-\tau^2})|}{|1-\tau^2| + |\sinh^2(\delta\sqrt{1-\tau^2})|},$$

(32)

where

$$\gamma^2 \Theta^2 = y^2 + 4\gamma^2 \theta'^2,$$

$$\tau_\pm = \frac{g^2}{2\omega_g^2}\left(1 + \frac{2\theta' \pm \Delta\theta_\parallel}{\varphi} - \frac{\omega}{\omega_{\mathrm{B}}}\right).$$

(33)

The universal function $Q^{\mathrm{br}}(\omega/\omega_{\mathrm{B}})$, calculated for fixed parameters δ, $2\gamma\theta'$, $L\langle n\rangle / L_{\mathrm{sc}}$ and different values of the parameter $\Delta\theta_\parallel/\varphi$, is presented in Fig. 4. Presented curves demonstrate essential spreading of the emission spectral width when increasing the collimator angular size $\Delta\theta_\parallel$ and decreasing the reflecting angle φ. It is interesting to note that the amplitude of the spectral distribution (32) is saturated with increasing of the parameter $\Delta\Theta_\parallel/\varphi$
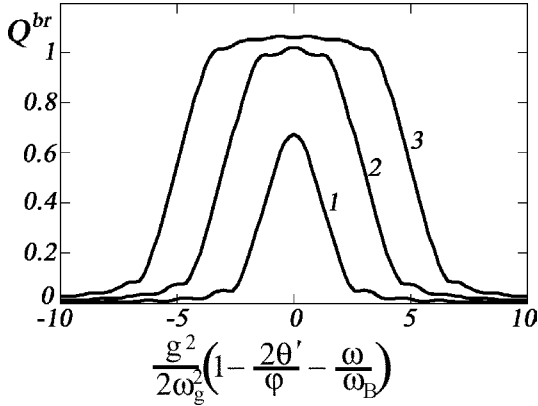
Fig. 4. The bremsstrahlung spectrum versus the photon collimator angular size. Here $\omega \frac{dN^{br}}{d\omega} = \frac{2e^2\omega_g^2\gamma\varphi}{\pi^2 g^2} Q^{br}$, the curves have been calculated for fixed values of the parameters $L\langle n\rangle/L_{sc} = 1$, $\theta' = 0$ and different values of the parameter $\frac{g^2\Delta\theta_\parallel}{2\omega_g^2\varphi} = 1$ (curve 1), 3 (curve 2) and 5 (curve 3).

and the subsequent growth of the emission yield is attended by spreading of the spectral width.

The tuning of the bremsstrahlung spectrum by the change of the orientation angle Θ' is demonstrated by the curves presented in Fig. 5.

An important advantage of a thin bremsstrahlung source over that of parametric radiation from X-mirror [9], is that the substrate of the X-mirror, used as monochromator in the bremsstrahlung
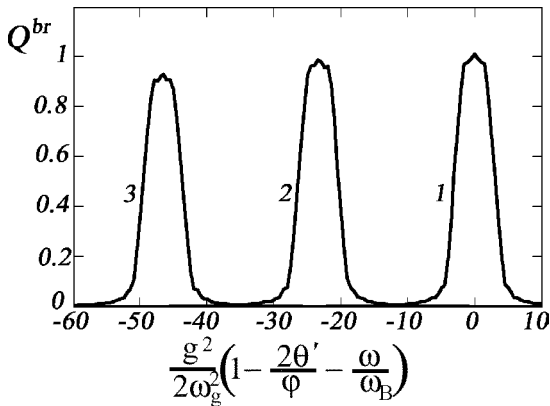

Fig. 5. The bremsstrahlung spectrum versus the orientation angle θ'. The curves have been calculated for fixed values of the parameters $L\langle n\rangle/L_{sc} = 1$, $\frac{g^2\Delta\theta_\parallel}{2\omega_g^2\varphi} = 3$, $\frac{\omega_g^2\gamma\varphi}{g^2} = 0.003$ and different values of the parameter $\gamma\theta' = 0$ (curve 1), 0.07 (curve 2) and 0.14 (curve 3).

case, can be thick since emitting electrons do not interact with the X-mirror; whereas, the substrate must be as thin as possible for the parametric X-ray source when it is an the internal target.

4. X-ray source based on the diffracted transition radiation

Returning to the general formula (15), let us consider an emission from electrons with high energies $\epsilon = \gamma m > m\omega/\omega_0$ ($\epsilon \geqslant 1$ GeV in the hard X-ray range where ω of the order of tens keV and $\epsilon \geqslant 100$ MeV in the soft X-ray range $\omega \sim 1$ keV). On condition of small enough thickness of internal target $L < L_{sc}$ under consideration the main contribution to total emission yield in the range $\omega \leqslant \gamma\omega_0$ makes the transition radiation mechanisms [20]. Ignoring as before the multiple scattering during the passage of the internal target, one can obtain from (15) the following expression for an emission amplitude:

$$
A_\lambda^{tr} = \frac{e}{\pi}\Omega_\lambda \left(\frac{1}{\gamma^{-2} + \Omega^2} - \frac{1}{\gamma^{-2} - \chi + \Omega^2} \right)
$$
$$
\times \left(1 - e^{-\frac{i\omega L}{2}(\gamma^{-2} - \chi + \Omega^2)} \right) R_\lambda, \tag{34}
$$

where $\chi = -\omega_0^2/\omega^2 + i\chi''$, the remaining quantities in (34) have been defined above.

Using (34) and repeating the calculations performed in the previous section, one can obtain the formula for the spectral–angular distribution of diffracted transition radiation:

$$
\omega \frac{d^3 N_\lambda^{tr}}{d\omega\, d^2\Theta} \approx \frac{2e^2\gamma^2 L_{sc}}{\pi^3 L} \int d^2\Psi K_0 \left(2\sqrt{\frac{\gamma^2\Psi^2 L_{sc}}{L\langle n\rangle}} \right)
$$
$$
\times \Omega_\lambda^2 \left(\frac{1}{\gamma^{-2} + \Omega^2} - \frac{1}{\gamma^{-2} + \frac{\omega_0^2}{\omega^2} + \Omega^2} \right)^2
$$
$$
\times \left(1 + e^{-L/L_{ab}} - 2e^{-L/2L_{ab}} \right.
$$
$$
\left. \times \cos\frac{\omega L}{2}\left(\gamma^{-2} + \frac{\omega_0^2}{\omega^2} + \Omega^2 \right) \right) |R_\lambda|^2, \tag{35}
$$

analogous to the result (27) and (30). Here $L_{ab}^{-1} = \omega\chi''$, $|R_\lambda|^2$ is defined by (22).

We shall restrict our consideration to electrons of very high energies (or photons of small energies), when $\gamma \gg \gamma_* = \omega_B/\omega_0$ and, therefore, the transition radiation yield peaks in the frequency range close to ω_B. In accordance with (35) the influence of multiple scattering on the interference between transition radiation waves emitted from the entrance and exit surfaces of the internal target is small with the understanding that

$$\frac{\omega L}{2}\langle\Psi^2\rangle \sim \frac{\omega_B L}{2\gamma^2}\frac{L\langle n\rangle}{L_{sc}} \ll 1. \tag{36}$$

Assuming the condition (36) to be fulfilled, one can obtain from (35) the following expressions for the diffracted transition radiation angular density

$$\frac{d^2 N_\lambda^{tr}}{d^2\Theta} \approx \frac{4e^2\omega_g^2\gamma^2}{\pi g^2}\tanh(\delta_\lambda)\alpha_\lambda\Phi_\lambda^{tr},$$

$$\Phi_\lambda^{tr} = \frac{L_{sc}}{L}\left(1 + e^{-L/L_{ab}} - 2e^{-L/2L_{ab}}\cos\frac{\omega_B L}{2}(\gamma^{-2} + \gamma_*^{-2} + \Omega^2)\right)$$

$$\times \int_0^\infty dt\, t K_0\left(2\sqrt{\frac{L_{sc}}{L\langle n\rangle}}t\right)\left(\frac{1}{2\gamma^2\Theta^2}\left(1 - \frac{\Theta_\lambda^2}{\Theta^2}\right)\right.$$

$$\times \left(\frac{1 + t^2 + \gamma^2\Theta^2}{\sqrt{(1+t^2+\gamma^2\Theta^2)^2 - 4t^2\gamma^2\Theta^2}} - 1\right)$$

$$\left. + 2\frac{\Theta_\lambda^2}{\Theta^2}\frac{t^2 + \gamma^2\Theta^2 + (t^2 - \gamma^2\Theta^2)^2}{((1+t^2+\gamma^2\Theta^2)^2 - 4t^2\gamma^2\Theta^2)^{\frac{3}{2}}}\right), \tag{37}$$

where the angle Θ is defined by (28). Note, the interference factor in (37) give us a possible method to achieve the maximum emission yield under conditions of positive interference: $\frac{\omega_B L}{2}(\gamma^{-2} + \gamma_*^{-2} + \Theta^2) \approx \frac{\omega_B^2 L}{2\omega_B} = \pi$. This interference is suppressed in circumstances where the inequality contrary to (36) is fulfilled. On condition under consideration the rapidly oscillating function $2e^{-L/2L_{ab}}\cos\frac{\omega L}{2}(\gamma^{-2} + \frac{\omega_0^2}{\omega^2} + \Omega^2)$ can be neglected in (35) and consequently the analogous term in (37) can be neglected as well.

Let us consider the dependence of the angular density of diffracted transition radiation on the average number of passes $\langle n\rangle$ and the thickness of the internal target L. In accordance with (37), the function $\Phi_\lambda^{tr}(\langle n\rangle)$ is a monotonically increasing

function, which is saturated in the range $\langle n\rangle > L_{sc}/L$. From the comparison between the functions Φ^{br} and Φ_λ^{tr} it may be concluded that the dependence of the emission angular density on $\langle n\rangle$ for diffracted bremsstrahlung and transition radiation is approximately the same.

On the other hand the dependence $\Phi_\lambda^{tr}(L)$ does not coincide with $\Phi^{br}(L)$, which is to say that the transition radiation yield from a target is not proportional to the thickness of this target. One can see that L-dependence of Φ_λ^{tr} is not determined by the single parameter $L\langle n\rangle/L_{sc}$ in contrast with Φ^{br}, but such a dependence takes place for the function $\Phi^{tr}/\langle n\rangle$ for the conditions $L \ll L_{ab}$ and $L \approx 2\pi\omega_B/\omega_0^2$ (resonance condition) under consideration. The dependence of the function $\Phi^{tr}/\langle n\rangle = (\Phi_1^{tr} + \Phi_2^{tr})/\langle n\rangle$ on the parameter $L\langle n\rangle/L_{sc}$ is illustrated by the curves presented in Fig. 6. The average angular density of transition-radiation photons decreases with the increasing of the parameter $L\langle n\rangle/L_{sc}$. The growth of the yield in center of the angular distribution is due to multiple scattering of the emitting particles. Note, the quantity $\langle n\rangle$ decreases with increasing L, and therefore the function Φ^{tr} decreases faster than $\Phi^{tr}/\langle n\rangle$.

It is interesting to compare the angular densities of X-ray sources based on the bremsstrahlung and the transition radiation. Using the formula (37), the curves in Fig. 6 and the parameters identical to
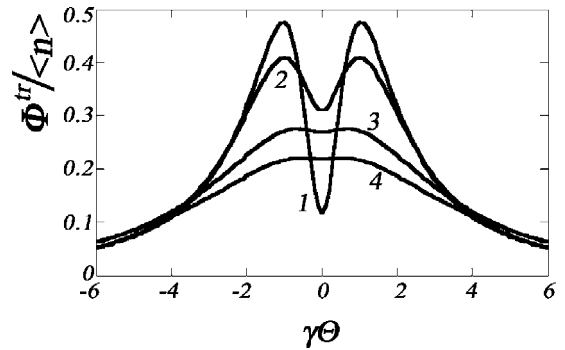

Fig. 6. The transition radiation angular distribution. Here $\frac{d^2 N^{tr}}{d^2\Theta} = \frac{4e^2\omega_g^2\gamma^2}{\pi g^2}\Phi^{tr}$. The curves have been calculated for different values of the parameter $L\langle n\rangle/L_{sc} = 0.1$ (curve 1), 1 (curve 2), 10 (curve 3) and 20 (curve 4).

that for the bremsstrahlung radiator, we obtain the following estimation: $dN^{tr}/d^2\Theta \approx 10$ ph./el.ster. This estimation exceeds essentially that obtained above for the scheme based on diffracted bremsstrahlung radiator. But one should take into account that in conditions where the energy of emitting particles are the same for both schemes considered the energies of emitted photons are very different. Indeed, the Bragg frequency ω_B must be much less than $\gamma\omega_0$ for transition radiation radiator but this frequency must be much more than $\gamma\omega_0$ for diffracted bremsstrahlung radiator in accordance with assumptions used in the performed analysis. In the case considered the average energy of emitted transition radiation photons must be much less than 2 keV. In these conditions photoabsorption can suppress the contribution of transition radiation waves emitted from in-surface of the target to total emission yield and therefore above estimation must be reduced by a factor of four. Thus, X-ray source based on the transition radiation radiator is of prime interest for soft X-ray producing.

To describe the spectrum of discussed emission, it is necessary to integrate the expression on the right-hand side of Eq. (35) over observation angles $\Theta_\perp$ and $\theta_\parallel$. The result of such integration has the form

$$\omega\frac{dN^{tr}_\lambda}{d\omega} \approx \frac{4e^2\omega_g^2\gamma\tan(\varphi/2)\alpha_\lambda}{\pi^2 g^2}Q^{tr}_\lambda,$$

$$Q^{tr}_\lambda = \int_{-\infty}^{+\infty}dy\,\Phi^{tr}_\lambda\int_{\tau_{\lambda-}}^{\tau_{\lambda+}}\frac{d\tau|\sinh^2(\delta_\lambda\sqrt{1-\tau^2})|}{|1-\tau^2|+|\sinh^2(\delta\sqrt{1-\tau^2})|},$$

$$\tau_{\lambda\pm} = \frac{g^2}{2\omega_g^2\alpha_\lambda}\left(1+\frac{2\theta'\pm\Delta\theta_\parallel}{2\tan(\varphi/2)}-\frac{\omega}{\omega_B}\right),$$

$$(38)$$

analogous to (32) and (33). Here $\gamma\Theta_1 = y$, $\gamma\Theta_2 = 2\gamma\theta'$ as before.

The function $Q^{tr}/\langle n\rangle = (Q^{tr}_1 + Q^{tr}_2)/\langle n\rangle$ has been calculated for fixed values of the parameters δ, $2\gamma\theta'$, $L\langle n\rangle/L_{sc}$ and different values of the parameter $\Delta\theta_\parallel/\varphi$. Results of calculations analogous to that obtained for the case of diffracted bremsstrahlung radiator are not presented here.

Formulae (37) and (38) allow us to describe all diffracted transition radiation characteristics of interest for the task of an effective X-ray source creation.

It should be remembered that the field of the application of these formulae is bounded by the used condition $\gamma \gg \gamma_*$, or $\omega_B \ll \gamma\omega_p$.

5. X-ray source based on the diffracted coherent bremsstrahlung

Let us consider the possibility of increasing the X-ray emission yield using coherent bremsstrahlung from a crystalline internal target. It should be noted that channeling radiation occurs simultaneously with coherent bremsstrahlung in the case under study, but the contribution of this radiation is small in the range of low energies of emitted photons to the left of the characteristic maximum in channeling radiation spectrum. We assume that the momentum of the electron beam is oriented at the small angle Ψ relative to the axis of atomic strings in a crystal and that its component in the plane perpendicular to the string's axis is placed far from the main directions of planar channeling. Since an emitting electron suffers accidental collisions with different atomic strings under discussed conditions [18], the spectral–angular distribution of the emission intensity can be defined as [18]

$$\frac{d^3N^{cb}_\lambda}{dt\,d\omega\,d\Omega} = n_0 a\Psi\int_{-\infty}^{+\infty}db\frac{d^2N^{str}_\lambda}{d\omega\,d\Omega},\qquad(39)$$

where n_0 is the density of atoms in internal target, a is the distance between atoms in an atomic string, $d^2N^{str}_\lambda/d\omega\,d\Omega$ is the distribution of coherent bremsstrahlung from relativistic electron on a single atomic string, integration in (39) is performed over all possible impact parameters b, determining the collision of an emitting particle with atomic string.

To determine the quantity $d^2N^{str}_\lambda/d\omega\,d\Omega$, we will use the formula (16) with σ_x instead of σ_0. Such an approximation is realistic because the photon formation length $l_{coh} \approx 2\gamma^2/(1+\gamma^2\omega_0^2/\omega^2)\omega$ is

much less than the thickness of internal target L. In addition to this it is suggested that the angle of an emitting electron scattering on an atomic string $\Delta\Psi \sim \sqrt{\Psi^2 + \Psi_c^2} - \Psi$ (Ψ_c is the critical channeling angle) is less than the characteristic angle of photon emission by a relativistic particle γ^{-1}. In this case the dipole approximation for the photon emission is valid. Assuming that atomic strings are oriented along the axis $\mathbf{e}_1$ (see Fig. 1), one can define the velocity of emitting electrons by the formula (17), where the scattering angle $\mathbf{\Psi}$ is changed in the process of coherent azimuthal scattering of an electron in the average string's potential [18]. Obviously, the formula (18) is appreciable for the description of coherent bremsstrahlung description as well, but some changes are required in this formula: $\gamma^{-2} \to \gamma^{-2} + \gamma_*^{-2}$, $\Psi_\perp \to \Psi\sin\eta$, $\Psi_\parallel \to \Psi\cos\eta$, η is the angle of coherent azimuthal scattering of an electron on atomic strings.

The components of electron acceleration W_z and W_x' coming into existence when such an electron moves in the average string potential can be determined by the expression

$$\mathbf{W}_\perp = \frac{2\pi ie}{m\gamma a} \int d^2 k_\perp \mathbf{k}_\perp \varphi_{-\mathbf{k}_\perp}$$
$$\times \exp\left(-\frac{1}{2}k_\perp^2 u_T^2 - i\mathbf{k}_\perp \mathbf{b} - i\mathbf{k}_\perp \mathbf{\Psi}t\right), \quad (40)$$

analogous to (19). Here u_T is the mean square amplitude of thermal vibrations of the target's atoms, $\mathbf{k}_\perp = \mathbf{e}_z k_z + \mathbf{e}_x' k_x'$, $\mathbf{b\Psi} = 0$.

Note, the approximation of rectilinear motion of an emitting electron through average string's potential is valid on condition $\Psi^2 \gg \Psi_c^2$ only. This condition restrains the field of application of this work. On the other hand, such a condition is necessary to obtain the emission yield in the soft X-ray range because this yield becomes small due to the formation of a maximum in the spectrum of both above-barrier and channeling electrons moving in a crystal at small angles $\Psi \leqslant \Psi_c$ to the string's axis [18].

Using (40) and modified formulae (18), one can obtain the following expression for $d^3 N_\lambda^{str}/d\omega d^2\Theta$:

$$\omega \frac{d^3 N_\lambda^{str}}{d\omega d^2\Theta} = |d_\lambda|^2 |R_\lambda|^2,$$

$$d_1 = \frac{4\pi ie^2}{m\gamma a\Psi} \frac{1}{\gamma^{-2} + \gamma_*^{-2} + \Omega^2} \int dk_1 \varphi_{-\mathbf{k}_\perp} e^{-\frac{1}{2}k_\perp^2 u_T^2 - ik_1 b}$$

$$\times \left[\left(1 - \frac{2\Omega_1^2}{\gamma^{-2} + \gamma_*^{-2} + \Omega^2}\right) k_z - \frac{2\Omega_1\Omega_2}{\gamma^{-2} + \gamma_*^{-2} + \Omega^2} k_x'\right],$$

$$d_2 = \frac{4\pi ie^2}{m\gamma a\Psi} \frac{1}{\gamma^{-2} + \gamma_*^{-2} + \Omega^2} \int dk_1 \varphi_{-\mathbf{k}_\perp} e^{-\frac{1}{2}k_\perp^2 u_T^2 - ik_1 b}$$

$$\times \left[\left(1 - \frac{2\Omega_2^2}{\gamma^{-2} + \gamma_*^{-2} + \Omega^2}\right) k_x' - \frac{2\Omega_1\Omega_2}{\gamma^{-2} + \gamma_*^{-2} + \Omega^2} k_z\right],$$
$$(41)$$

where the following designations are used:

$$k_\perp^2 = k_1^2 + k_2^2, \quad k_2 = \frac{\omega}{2\Psi}(\gamma^{-2} + \gamma_*^{-2} + \Omega^2),$$
$$k_z = k_1\cos\eta + k_2\sin\eta, \quad k_x' = -k_1\sin\eta + k_2\cos\eta.$$
$$(42)$$

Let us consider the possibility of producing hard X-rays from coherent bremsstrahlung. Assuming the reflection angle φ to be small and substituting (41) and (42) to (39) one can obtain after integration over impact parameters b and summation over polarizations the following expression for the coherent bremsstrahlung spectral–angular distribution

$$\omega \frac{d^3 N^{cb}}{dt\, d\omega\, d^2\Theta} = \frac{4Z^2 e^6 n_0}{\pi m^2 \gamma^2} \frac{R}{a\Psi}$$

$$\times \left(1 - \Phi\left(\frac{u_T}{R}\right) - \frac{2u_T}{R\sqrt{\pi}} e^{-\frac{u_T^2}{R^2}}\right)$$

$$\times \left\langle \frac{1}{(\gamma^{-2} + \gamma_*^{-2} + \Omega^2)^2} \left[1 - \frac{4(\gamma^{-2} + \gamma_*^{-2})}{(\gamma^{-2} + \gamma_*^{-2} + \Omega^2)^2} \right.\right.$$

$$\left.\left. \times (\Omega_1\cos\eta - \Omega_2\sin\eta)^2\right]\right\rangle (|R_1|^2 + |R_2|^2).$$
$$(43)$$

Obviously, the main difference between the coherent bremsstrahlung intensity (43) and that of the ordinary bremsstrahlung (20) consists in the coefficient $R/a\Psi$. This coefficient shows the number

of atoms in an atomic string making a coherent contribution to the formation of the bremsstrahlung yield [18]. The value of this coefficient can be large for small enough incidence angles $\Psi \ll R/a$, so that the use of crystalline radiators allows us to increase the bremsstrahlung yield very essentially. This theoretical conclusion is in agreement with experimental results [13,14] consisting in the observation of the increase in X-ray yield from 500 MeV electron beam crossing Si crystalline radiator in comparison with amorphous one (a tenfold increase of the yield in X-ray range has been observed). On the other hand, such effect can be realized with the proviso that the emission formation length l_{coh} exceeds the electron path in the atomic string potential R/Ψ. This condition sets limits on the possible photon energies

$$\omega \approx \omega_{\mathrm{B}} \ll \frac{2\gamma^2 \Psi}{R}. \tag{44}$$

The further calculations are analogous to that performed above and are not presented here. It should be noted that the multiple scattering of the emitting electrons is more complicated in the case being considered and includes both coherent azimuthal scattering on the average potential of atomic strings (the value of incidence angle Ψ is preserved in this process) and incoherent scattering appearing due to thermal vibrations of atoms (this scattering changes the incidence angle Ψ). The distribution function taking into account both these processes has been obtained in [21].

6. Conclusions

A thin internal target inside a cyclical accelerator and an external X-mirror make a promising source of x-rays having some advantages over that of an internal X-mirror. Since emitting electrons do not interact with X-mirror, small incidence angles of the photons relative to X-mirror reflecting plane are possible, which becomes important for hard X-ray emission. The thickness of the substrate in the external X-mirror can be arbitrary for the same reason.

The three radiators were considered in this work: bremsstrahlung, transition radiation and coherent bremsstrahlung radiators, each having advantages and disadvantages of their own.

The bremsstrahlung radiator best suited to produce X-rays in the region $\omega \gg \gamma\omega_0$ allows to use electron beams with relatively small energies (e.g. 10–30 MeV) for hard X-ray generation (ω of the order of tens keV). The estimation of the angular density of emitted by 30 MeV electron beam X-rays shows the possibility to achieve the value of the order of 0.1–0.2 ph./el.ster., two order more than that achievable in a single passage of electrons through crystalline or multilayer radiators. In line with performed calculations, the maximum possible emission angular density is bounded in the main by the influence of multiple scattering of emitting electrons. Because of this it may be advantageous to use the internal target based on light elements.

More intensive source can be created on the basis of coherent bremsstrahlung radiator. The emission yield from such a radiator can be increased by a factor of $R/a\Psi \gg 1$ (the increase in X-ray yield from crystalline radiator by a factor of 8 in comparison with amorphous target has been observed experimentally [13,14]), but the range of emitting photons is limited in the case in question by the condition $\omega \ll 2\gamma^2 \Psi/R$.

The transition radiation is of prime interest for soft X-ray producing in the range $\omega \ll \gamma\omega_0$. The possibility to obtain the photon beams with angular density of the order of 10 ph./el.ster. has been shown in the paper. An important point is that this density can be obtained by the use of electron beam with relatively small energy of the order of 30 MeV, but the energy of emitted photons is less than 1 keV in the case considered. High energy electron beams (e.g. hundreds MeV) are needed to produce X-rays in the range of tens keV by the method considered.

The derived expressions for angular and spectral distributions take into account both the emitting particle losses during multiple passes through an internal target and the multiple scattering of such particles. These expressions allow us to calculate most of the needed characteristics of these X-ray sources.

Acknowledgements

References

[1] M.Yu. Andreyashkin, V.V. Kaplin, M.A. Piestrup, S.R. Uglov, V.N. Zabaev, Appl. Phys. Lett. 72 (1998) 1385.

[2] V.V. Kaplin, S.R. Uglov, O.F. Bulaev, V.J. Goncharov, M.A. Piestrup, C.K. Gary, Nucl. Instr. and Meth. B 173 (2001) 3.

[3] M.A. Piestrup, L.W. Lombardo, J.T. Cremer, G.A. Retzlaf, R.M. Silzer, D.M. Skopik, V.V. Kaplin, Rev. Sci. Instr. 69 (1998) 2223.

[4] M.L. Ter-Mikaelian, High Energy Electromagnetic Processes in Condensed Media, Wiley, New York, 1972.

[5] V.G Baryshevskiy, I.D. Feranchuk, Sov. Phys. JEPT 34 (1972) 495.

[6] G.M. Garibian, S. Yang, Sov. Phys. JEPT 34 (1972) 502.

[7] A. Caticha, Phys. Rev. A 40 (1989) 4322.

[8] N. Zhevago, Proc. II Symp. on Transition Radiation of High Energy Particles, Yerevan, Armenia, 1983, p. 200.

[9] V.V. Kaplin, S.R. Uglov, V.N. Zabaev, M.A. Piestrup, C.K. Gary, N.N. Nasonov, M.K. Fuller, Appl. Phys. Lett. 76 (2000) 3647.

[10] B. Pardo, J.-M. Andre, Phys. Rev. E 65 (2002).

[11] N.N. Nasonov, V.V. Kaplin, S.R. Uglov, M.A. Piestrup, C.K. Gary, Phys. Rev. E 68 (2003) 36504.

[12] N.K. Zhevago, V.I. Glebov, Phys. Lett. A 309 (2003) 311.

[13] B.N. Kalinin, G.A. Naumenko, D.V. Padalko, A.P. Potylitsin, I.E. Vnukov, Nucl. Instr. and Meth. B 173 (2001) 253.

[14] E. Bogomazova, B.N. Kalinin, G.A. Naumenko, D.V. Padalko, A.P. Potylitsyn, A.F. Sharafutdinov, I.E. Vnukov, Nucl. Instr. and Meth. B 201 (2001) 276.

[15] Z.G. Pinsker, Dynamical Scattering of X-rays in Crystals, Springer, Berlin, 1981.

[16] U. Arkatov, S. Blazhevich, G. Bochek, E. Gavrilichev, A. Grinenko, V. Kulibaba, N. Maslov, N. Nasonov, V. Pirogov, Y. Virchenko, Phys. Lett. A 219 (1996) 355.

[17] N.N. Nasonov, Nucl. Instr. and Meth. B 173 (2001) 203.

[18] A.I. Akhiezer, N.F. Shulga, High Energy Electrodynamics in Matter, Gordon and Breach, London, 1996.

[19] V.I. Bespalov, V.V. Kashkovsky, V.L. Chakhlov, Nucl. Instr. and Meth. B 201 (2003) 292.

[20] V.L. Ginzburg, I.M. Frank, J. Phys. (Moscow) 9 (1945) 353.

[21] A.A. Grinenko, N.N. Nasonov, V.D. Tsukanov, Zh. Tech. Fiz. 61 (1991) 185.